Strength of Faults and Maximum Stress-drops in Earthquakes

Christopher H. Scholz
Lamont-Doherty Earth Observatory,
Columbia Univ., Palisades, New York, 10964

Abstract

We investigate the strength of rock at the field scale and the maximum stress-drop that can occur within earthquakes by studying the displacement profiles of faults and earthquakes. The displacement to length ratio D/L is in the range of 10^{-3} – 10^{-2} for faults, indicating stress-drops in the range 1 – 10 kb. These depend on lithology, with faults in sedimentary rocks at the lower end of the range and those in crystalline basement at the upper end. The D/L range for large earthquakes is 10^{-5} – 10^{-4}, corresponding to stress-drops in the range 10 – 100 bars. Earthquakes and faults both tend to have linear displacement tapers near their tips. The magnitude of tip tapers indicate the rupture resistance near the propagating tip. For isolated faults and earthquakes the tip tapers (which are scale independent) have values that track with the D/L ratios of the corresponding rupture. However, the tip tapers can be as much as an order of magnitude higher when the rupture tip interacts with the stress field of an adjacent rupture tip. For earthquakes, this indicates that stress-drops can locally be as high as a kb at such interacting regions as interior fault jogs, where the rupture encounters the end of the fault, or when the rupture tip enters the stress shadow of a previous earthquake.

Introduction

Two issues are addressed here, the strength of rock at the field scale and the maximum stress-drop that can occur within earthquakes. The approach is to study the displacement profiles of faults and earthquakes. The displacement amplitudes of faults scale linearly with length, the ratio of the two, D/L, is proportional to stress-drop, (σ_y - σ_f), . where σ_y is the yield strength of the rock and σ_f is the residual friction. The displacement gradients near the tips of earthquakes and faults are, generally, approximately linear. This feature is one of the predictions of the CFTT (critical fault tip taper) model, an elastic-plastic crack model that best agrees with fault observations (Scholz, 2002, pp. 16-17 and 115-121). In this model (the application to shear cracks of the CTOA model for Mode I cracks, see Kanninen and Popelar, 1985), the material in a volume around the fault tip is allowed to yield inelastically wherever the yield strength σ_y is exceeded. the CFTT is proportional to the stress-drop at the tip of the fault, and hence measures the local rupture resistance. In the case of an earthquake, D/L and CFTT are correspondingly proportional to the friction stress-drop (μ_s - μ_d) σ_n. The CFTT, which measures a local stress drop, and D/L, which measures the mean stress drop, will not indicate the same stress drop value unless the rupture has propagated in uniform rock in a uniform stress field.

There are a number of predictions the model makes regarding CFTT. If the crack (fault or earthquake) propagated in a uniform rock and stress field, it would remain

constant during propagation, i.e., CFTT is scale independent (see Newman et al., 2003). However, because strength depends on lithology but friction does not (Byerlee, 1978), CFTT should depend on rock type for faults but not for earthquakes.

Mean Stress-drop of Faults and Earthquakes

In both cases the scaling relationship between D and L is linear, as shown in Fig. 1, but with very different scaling parameters. The D/L ratio for large earthquakes range from 10^{-5} - 10^{-4}, corresponding to stress-drops of 10-100 bars. The primary systematics in this variation is between interplate and intraplate earthquakes, the latter having stress-drops averaging about 4 times higher than of the former (Scholz, 2002, p. 206-207). The faults have much higher D/L ratios, in the range of 10^{-3} - 10^{-2}, corresponding to stress-drops of 1-10 kb. These therefore represent lower bounds for the strength of rock at the field scale. In this case the variation correlates with lithology, the smaller D/L values are for small faults in sedimentary rocks and the larger ones for faults in crystalline basement. The conclusion is that the stress-drops for faults are typically two orders of magnitude greater than those for earthquakes. One of the questions we will ask is: can the local stress-drop within an earthquake be as high as the rock strength?

Fault and Earthquake Tip Tapers and Local Stress-drops

Figure 2 shows the displacement profiles for a number of isolated normal faults in the Volcanic Tablelands, eastern California, normalized to fault length. These faults range in length from 690-2200 m, and the good data collapse in Fig. 2 indicates that self-similarity extends to the entire profile, not just maximum displacement as indicated in Fig. 1. Notice that the tip taper is scale-independent, as expected from the CFTT model.

FTTs (fault tip taper, the measured quantity, corresponds to CFTT only when it is measure along the centerline of a fault in a uniform rock type) are strongly dependent on stress interactions between faults and between earthquakes. For faults, the most common form of such interactions is when sub-parallel faults or fault segments overlap, such that the interacting tips lie within the stress shadows of the adjacent fault. The displacement profiles in such cases become asymmetric, in which the peak slip region is shifted towards the interacting tip and the FTT at that end becomes steeper than that of the distal end (Peacock, 1991; Peacock and Sanderson, 1993; Contreras et al., 2000). This occurs because the FTT at the interacting tip must overcome both the rupture resistance and the stress-drop of the adjacent fault (Willemse et al., 1996; Willemse, 1997; Scholz, 2002, p. 127-129). The degree to which FTTs can be augmented by such interactions is highly variable: it depends on the offset and separation of the fault tips (Gupta and Scholz, 2000). We are interested in this topic because earthquakes are often highly segmented, and segment boundaries are where strong interactions take place and the stress-drops are likely to be highest. We can investigate this by studying the earthquake tip taper of such interior segments.

Figure 3a shows the FTTs for the faults in the Bishop (welded tuff) in the Volcanic Tablelands (Dawers et al., 1963. These are all along the fault centerlines and hence true CFTTS (Scholz and Lawler, 2004). Average FTT for other isolated faults range from $1x10^{-3}$ to $8x10^{-2}$ and increase with rock strength. FTTs for interacting faults average $1.2x10^{-1}$ with much more scatter.

Table 1. Summary of tip taper data.

Rupture type	Ave.FTT	S.D.
Isolated-all	3.8E-2	4.9E-2
Isolated-tuff	5.1E-2	2.1E-2
Isolated-granite	8.0E-2	7.6E-2
Isolated-seds.	1.1E-2	1.0E-2
Isolated-strikeslip	5.0E-2	4.5E-2
Isolated-normal	3.6E-2	4.9E-2
Interacting faults	1.2E-1	1.0E-1
Interior eqk	1.4E-3	1.3E-3
Exterior eqk.	1.8E-4	9.7E-5

The CFTTs for large earthquakes (those with lengths > 30 km, dashed line in Fig. 3b) are, like their D/L ratios, about 2 orders of magnitude smaller than those of faults, averaging 1.8×10^{-4}. Interior tips of earthquake segments have FTTs about an order of magnitude steeper than the exterior tips of earthquakes. The steepest one we measured, for the Lone Pine segment of the 1872 Owens Valley earthquake, was 5×10^{-3}, although that scarp was probably produced by three earthquakes (Lubitkin and Clark, 1988).

Examples of two types of earthquake interactions are shown in Figure 5. Figure 5a shows the slip distribution in the 1992 Landers earthquake on the Kickapoo fault, a 4 km long 'shunt' fault that runs obliquely through the extensional jog between the Johnson Valley fault and the Homestead Valley fault (Sowers et al., 1994). The strike-slip displacement goes to zero at each end of the Kickapoo fault and neither was mapped as touching the other two faults. This is thus an example of a strength barrier in which the rupture segment propagated to the ends of the fault, thereby encountering solid rock. The FTT at the north and south tip of the Kickapoo fault are 1.5 and 1.8×10^{-3}, respectively, a factor of 10 greater than the average value for non-interacting earthquake tips. The D/L ratio for the Kickapoo fault was about 5×10^{-3}, about 10 times higher than for the Landers earthquake as a whole, also indicating a kb stress-drop there. The Landers rupture was impeded for several seconds at this point (Wald and Heaton, 1994), and dynamic modeling indicated an unusually high stress-drop there (Olson et al., 1997). A second example of this type of barrier is found in the 1959 Hegben Lake earthquake. This earthquake had two rupture segments. The western end of the west segment reached the end of the fault. It had a taper of 4×10^{-3}, ten times larger than three other tips (Whitkind, 1964).

The second type of earthquake interaction, a relaxation barrier, is shown in Fig. 5b, where the surface displacement distributions for the 1940 and 1979 Imperial Valley earthquakes are plotted. Inversions of geodetic and seismic data indicated that the slip at depth in the northern part of both events were somewhat higher than the surface values, about a meter for the 1940 and about half that for the 1979 event, but the deep slip at the southern end of the 1940 rupture was similar to the surface displacement profile (King and Thatcher, 1998). The potential slip accumulated on the Imperial fault between 1940 and 1979 is shown by the horizontal line, based on the estimate of 35 ± 2 mm/yr from GPS data (Bennett et al., 1996). Hence the 1940 stress-drop had by 1979 been recovered in the northern end of the rupture but not in the southern end, where the slip was greater than the accumulation line, indicating that a residual stress-drop existed in that region in

1979. The 1979 earthquake ruptured the northern end of the 1940 rupture and then entered the stress shadow of the 1940 earthquake and abruptly stopped, with a high FTT of 1.6×10^{-3}, indicating the same type of interaction that has been observed for overlapping faults.

Discussion

The results above indicate that a minimum estimate for upper crustal strength is in the order of 10 kb. Earthquake stress-drops can reach a factor of 10 higher than mean stress-drops in locally, at fault segment boundaries. Faults in the vicinity of Yucca Mtn. are intraplate faults, so should be expected to have stress-drips on the order of 100 bars, so local stress-drops within them can reach a kb or so.

There are seismological observations of kb stress drops as well. Munguia and Brune, 1984) found kb stress drop sub-events in the 1980 Victoria, Mexico earthquake (M 6.1). Mori and Shimazaki (1984) interpreted strong motion records of the 1968 Tokachi-oki M 7.9 earthquake as indicating several very high stress-drop subevents (~ 4kb). A accelerometer at Cape Mendicino registered a high-frequency 2g acceleration from the 1992 Petrolia (M 7) earthquake, whereas the nearby (6 km) station recorded a maximum of only 0.6 g. Oglesby and Archuleta (1997), argued that this was a source effect and modelled it with as caused by the rupture of a high stress-drop asperity on this shallow dipping fault plane just below the Cape Mendicino station. They point out that this form of focusing can only occur along a normal from the fault plane connecting the asperity and station. Thus to determine whether of not such a focusing event can occur at Yucca Mountain, one needs to know the strike and dip of the nearby faults to see if a normal from the lower part of the fault plane (where such high strength features are likely to occur) can intersect the facility.

The results show that when earthquakes propagate to fault tips, their FTTs become an order of magitude larger than otherwise, but not the two orders of magnitude necessary to reach the rock strength there. However, faults grow incrementally, in earthquakes (Cowie and Scholz, 1993), as shown in a stepwise manner in Figure 6. At equilibrium the fault tip taper is CFTT (Fig. 6a). If an earthquake occurs on the fault and propagates to the fault's end, it will contribute its earthquake tip taper (ETT. Fig. 6b.). The fault responds by growing and increment ΔL to restore the CFTT (fig. 6c.. There is no need for the ETT to be as large as the CFTT: the examples given above indicate that it is about a tenth of that.

Figures

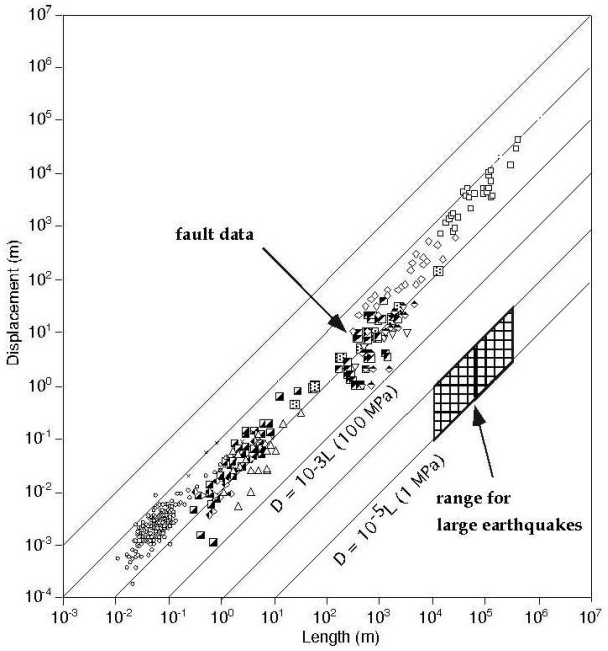

Figure 1. Scaling between displacement and length for earthquakes and faults. Fault data from Schlische et al., (1996).

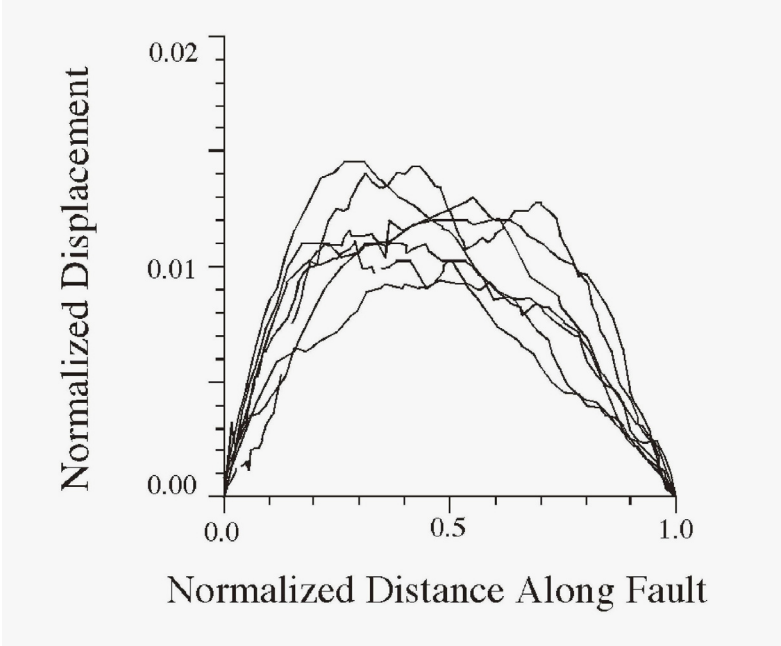

Figure 2. Displacement profiles normalized to fault length for isolated faults with lengths from 690 to 2200 m in the Volcanic Tablelands, California. Data from Dawers et al. (1993).

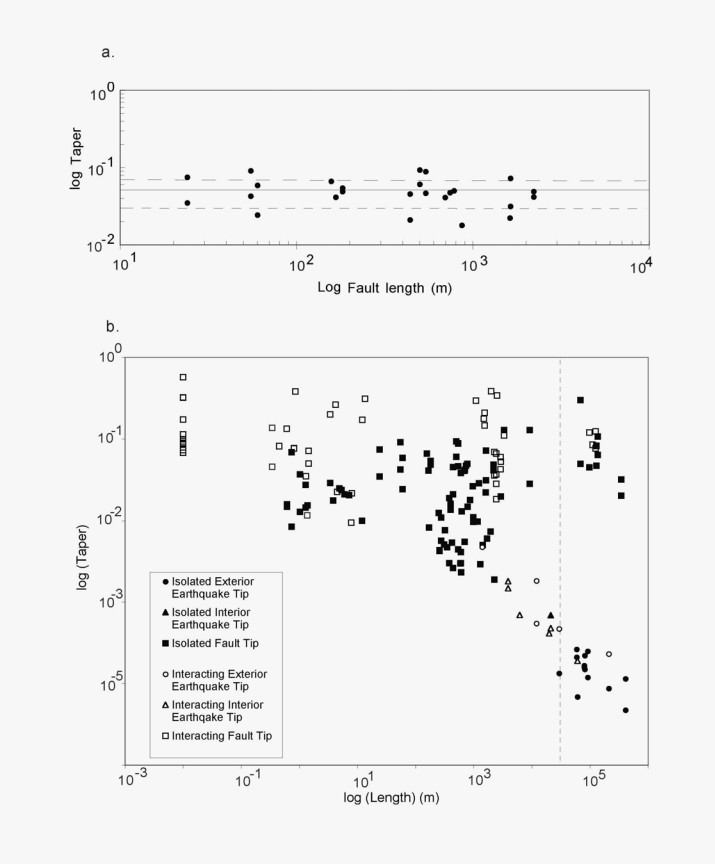

Figure 3. a) Fault tip tapers for a larger dataset of isolated faults in the Volcanic Tablelands (data from Dawers et al. (1993). b), tip tapers for a variety of faults and earthquakes (data from Scholz and Lawler, 2004).

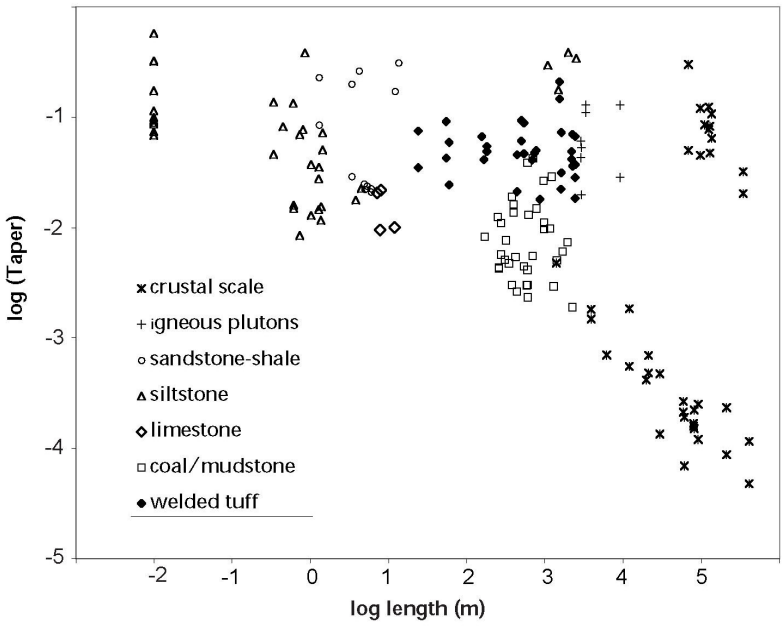

Figure 4. The same data as in Fig. 3b, sorted in terms of lithology (from Scholz and Lawler, 2004).

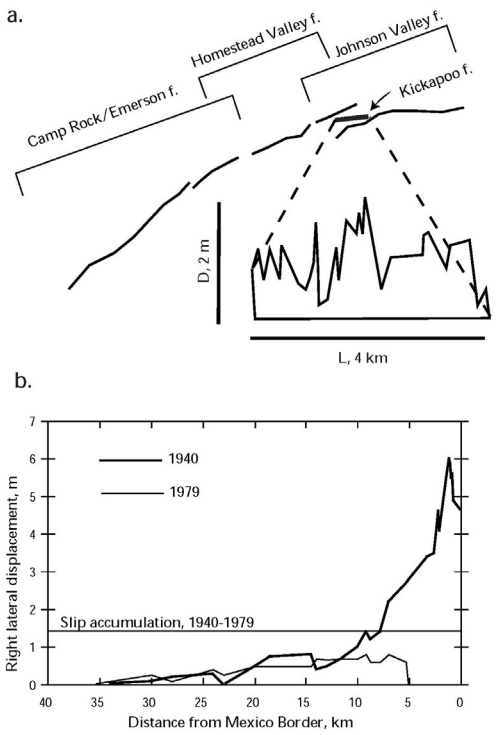

Figure 5. a) Slip distribution of the Kickapoo fault, linking the Johnson Valley faults and the Homestead Valley faults in the 1992 Landers earthquake (data from Sowers et al, 1994_.. b) Surface slip distributions in the 1940 and 1979 Imperial Valley earthquakes. (data from Sharp, 1982).

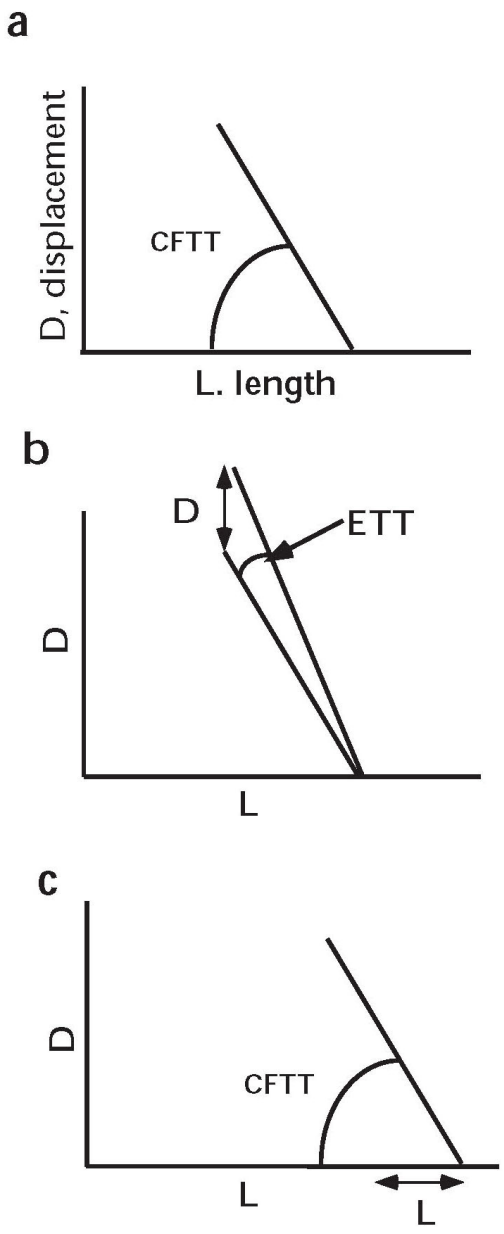

Fig. 6a shows the fault tip displacement taper at equilibrium, with the taper at the CFTT. In Fig. 6b, an earthquake has propagated to the end of the fault and added its increment of slip, □D, and earthquake tip taper ETT. In response, the fault then grows an increment □L to restore the taper to the CFTT. It is not necessary for the ETT to equal the CFTT (Cowie and Scholz, 1993). The ETT and its corresponding stress-drop is likely to be similar to what we have observed for interior earthquake segments, about a tenth of the rock strength.

References

Bennett, R A., W. Rodi, and R.E. Reilinger, Global Positioning System constraints on fault slip rates in southern California and northern Baja, Mexico, J. Geophys. Res. , 101, 21,943-21,960, 1996.

Byerlee, J. Friction of Rocks. Pure and Applied Geophy. 116: 615-626, 1978.

Contreras, J., M. H. Anders, and C. H. Scholz, Growth of a normal fault system: observations from the Lake Malawi basin of the east African rift. J. Struct. Geol. 22, 159-168 2000.

Cowie, P. A., and Scholz, C.H. Growth of faults by accumulation of seismic slip. *J. Geophys. Res.* **97(B7)**, 11085-11095 (1992b).

Dawers, N.H., M.H. Anders, and C.H . Scholz, Growth of normal faults: Displacement-length scaling. Geology 21: 1107-1110, 1993.

Gupta, A., and C.H. Scholz, A model of normal fault interaction based on observations and theory. J. Struct. Geol. 22: 865-879, 2000.

Kanninen, M. F. & Popelar, C. H. Advanced Fracture Mechanics , Oxford Univ. Press, Oxford, 1985.

King, N.E., and W. Thatcher, The coseismic slip distribution of the 1940 and 1979 Imperial Valley, California, earthquakes and their implications, J. Geophys. Res, 103, 18,069-18,086, 1998.

Lubetkin, L. K. C., and M. M. Clark, Late Quaternary activity along the Lone Pine fault, eastern California, Geol. Soc. Amer. Bull. 100, 755-766, 1988.

Newman, J. C., M. A. James, and U. Zerbst, A review of the CTOA/CTOD fracture criterion, Eng. Fracture Mech. 70, 371-385, 2003.

Mori, J. and Shimazaki, K., High stress-drops of of short period sub-events form the 1968 Tokachi-oki earthquakes as observed on strong ground motion records, Bull. Seismo. Soc. Am., 74, 1529-1544, 1984.

Munguia, L., and J. N. Brune, Simulations of strong ground motions for earthquakes in the Mexicali-Imperial Valley, Geophys. J. R. Astron. Soc., 79, 747-771, 1984.

Oglesby, D. D. and R.J. Archuleta, A faulting model for the 1992 Petrolia earthquake: Can extreme ground acceleration be a source effect?, J. Geophys. Res., 102, 11,877-11,897, 1997.

Olsen, K. B., R. Madariaga, and R. J. Archuleta, Three-dimensional dynamic simulation of the 1992 Landers earthquake. Science 278, 834-838, 1997.

Peacock, D.C.P. Displacements and segment linkage in strike-slip fault zones. J. Struct. Geol. 13: 1025-1035, 1991.

Peacock, D.C.P., and D.J. Sanderson, Displacements, segment linkage and relay ramps in normal-fault zones. J. Struct. Geol. 13: 721-734, 1991.

Schlische, R.W., S.S. Young, , R.V. Ackermann,., and A. Gupta, Geometry and scaling relations of a population of very small rift-related normal faults, Geology 24:683-686, 1996.

Scholz, C.H. 2002. The Mechanics of Earthquakes and Faulting, 2nd ed. Cambridge University Press:Cambridge, UK.

Scholz, C.H. and T.M. Lawler, Displacement tip tapers for faults and earthquake, sub. GRL, 2004.

Sharp, R.V. Comparison of 1979 surface faulting with earlier displacements in the Imperial Valley, in The Imperial Valley, California, earthquake of October 15, 1979, Geol. Surv. Prof. Paper 1254, p. 213-222, 1982.

Sowers, J.M., J.R. Unruh, W.R Lettis, and T.D. Rubin, Relationship of the Kickapoo fault to the Johnson Valley and Homestead Valley faults, San Bernardino County, California. Bull. Seis. Soc. Am. 84: 528-536, 1994.

Wald, D.J. and T.H. Heaton, Spatial and temporal distribution of slip for the 1992 Landers, California, Earthquake. Bull. Seis. Soc. Am. 84: 668-691, 1994.

Whitkind, I.J., in The Hebgen Lake, Montana Earthquake of August 17, 1959, pp 37-50, USGS Prof. Pap. 435, 1964.

Willemse, E.J.M.. Segmented normal faults: Correspondence between three dimensional mechanical models and field data. J.Geophys.Res.-Solid Earth 102: 675-692, 1997

Willemse, E.J.M., D.D. Pollard, and A. Aydin, Three-dimensional analyses of slip distributions on normal fault arrays with consequences for fault scaling. J.Struct.Geol. 18: 295-309, 1996.